Faraday Discussions

Multicomponent Supramolecular Hydrogels Composed of Cationic Phenylalanine Derivatives and Anionic Amino Acids

Journal:	*Faraday Discussions*
Manuscript ID	FD-ART-12-2024-000198.R1
Article Type:	Paper
Date Submitted by the Author:	19-Dec-2024
Complete List of Authors:	Ghosh, Shruti; University of Rochester, Chemistry Distaffen, Hannah; University of Rochester, Chemistry Jones, Christopher ; University of Rochester - River Campus, Nilsson, Bradley; University of Rochester, Department of Chemistry

Multicomponent Supramolecular Hydrogels Composed of Cationic Phenylalanine Derivatives and Anionic Amino Acids

*Shruti Ghosh,[a] Hannah E. Distaffen,[a] Christopher W. Jones,[a] and Bradley L. Nilsson[a,b]**

[a] Department of Chemistry, University of Rochester, Rochester, NY, 14627-0216, USA

[b] Materials Science Program, University of Rochester, Rochester, NY 14627-0166, USA

E-mail: bradley.nilsson@rochester.edu

Tel. +1 585 276-3053

ABSTRACT

Supramolecular hydrogels composed of self-assembled fluorenylmethoxycarbonyl phenylalanine (Fmoc-Phe) derivatives have been the focus of intense study as novel materials for biological applications that include drug delivery, tissue engineering, and regenerative medicine. Cationic Fmoc-Phe derivatives functionalized with diaminopropane (Fmoc-Phe-DAP) have been shown to undergo self-assembly and hydrogelation upon an increase in solution ionic strength by the addition of inorganic salts that provide cation-shielding counterions. Further, the identity of the inorganic salts modifies the assembly morphology and emergent viscoelastic properties of the resulting materials. Herein, we report multicomponent hydrogels composed of Fmoc-Phe-DAP derivatives in which hydrogelation is promoted by the addition of anionic amino acids, monosodium aspartate or monosodium glutamate. Aspartate and glutamate salts both support supramolecular gelation of Fmoc-Phe-DAP derivatives, although only the glutamate gels remain stable over periods longer than one hour. The assemblies formed by Fmoc-Phe-DAP derivatives in the presence of aspartate and glutamate are morphologically distinct relative to those formed in the presence of sodium chloride. The viscoelastic properties of stable glutamate/Fmoc-Phe-DAP derivative hydrogels are sensitive to the ratios of glutamate to Fmoc-Phe-DAP derivative, with

increased concentrations of glutamate corresponding to higher viscoelastic strength. These multicomponent systems demonstrate that comixing unfunctionalized amino acids with self-assembling Fmoc-Phe-DAP derivatives is yet another effective method to modify the emergent properties of the resulting materials.

1. INTRODUCTION

Hydrogels are valued biomaterials for applications that include drug delivery, tissue engineering, and regenerative medicine.[1-4] A broad range of polymer-derived hydrogels have been extensively used for these types of applications,[5-8] but many of these materials suffer from problems with biocompatibility and immunogenicity.[9] Supramolecular hydrogels composed of self-assembling proteins and peptides have been found to have improved emergent properties relative to non-natural polymer counterparts, including improved viscoelastic and thixotropic character and enhanced biocompatibility.[10-14] The high cost of synthetic peptides has been a barrier to the widespread adoption of supramolecular peptide hydrogels,[15-17] inspiring the development of more cost-effective low molecular weight (LMW) supramolecular hydrogels formulated from short self-assembling peptides (three amino acids or less in length) or modified amino acid derivatives.[18-25] Phenylalanine (Phe) and related aromatic amino acid derivatives are particularly effective as self-assembling hydrogel agents.[26-30]

Phe-derived hydrogels have been adopted both as models for the study of supramolecular self-assembly and hydrogelation and as materials for advanced biotechnology applications. Fluorenylmethoxy (Fmoc)-modified Phe derivatives have been extensively studied as hydrogel agents.[31-39] We have designed cationic derivatives of Fmoc-Phe in which the C-terminal carboxylic acid has been modified with diaminopropane (DAP) (**Figure 1**). Aqueous solutions of these Fmoc-Phe-DAP derivatives undergo spontaneous hydrogelation upon the addition of screening

counterions.[40] The properties of the resulting self-assembled hydrogels are sensitive to the side chain structure of the Phe derivative[41] and to the identity of the screening counterions, with differing structures and conditions affording unique self-assembled morphologies that include fibers, nanotubes, and amorphous aggregates that are self-supporting hydrogels, colloidal suspensions, or precipitates, respectively.[42] Among these Fmoc-Phe-DAP materials are hydrogels that exhibit ideal properties for sustained, localized drug delivery of both small molecule and protein cargo.[43, 44]

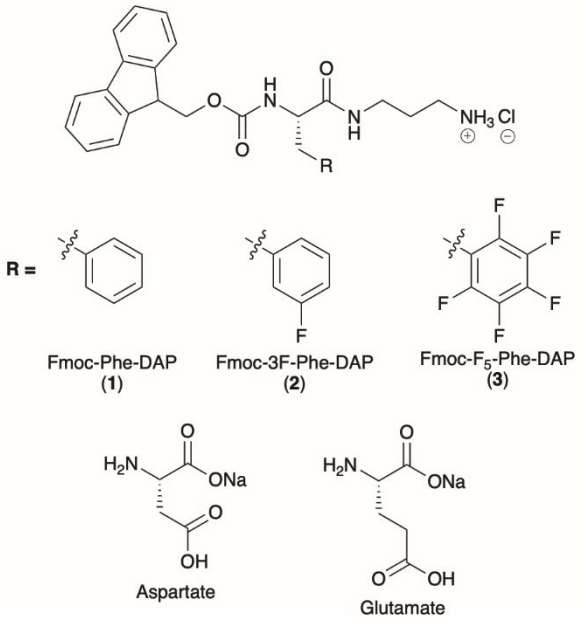

Figure 1. Chemical structures of cationic fluorenylmethoxy (Fmoc)- and diaminopropane (DAP)-modified phenylalanine derivatives and anionic amino acid gelation agents. Phenylalanine derivatives include phenylalanine (Fmoc-Phe-DAP, **1**), 3-fluorophenylalanine (Fmoc-3F-Phe-DAP, **2**), and pentafluorophenylalanine (Fmoc-F_5-Phe-DAP, **3**). Anionic amino acids in the monosodium salts of aspartic acid and glutamic acid.

Herein, we report the effect of anionic amino acids, glutamic acid and aspartic acid, as screening agents to promote the self-assembly and hydrogelation of Fmoc-Phe-DAP derivatives.

It has been demonstrated that coassembly of LMW amino acid derivatives with other agents often leads to the formulation of hybrid, multicomponent materials with unique and/or improved properties relative to the viscoelastic characteristics of hydrogels the individual components.[32, 33, 45-49]We hypothesized that cationic Fmoc-Phe-DAP derivatives would effectively assemble in the presence of anionic glutamate and aspartate salts as counterion partners to provide novel multicomponent hydrogel materials. Further, we also wished to understand the emergent morphological and viscoelastic properties of these coassembled hybrid hydrogel materials. Accordingly, we characterized the self-assembly and hydrogelation of aqueous solutions of three Fmoc-Phe-DAP derivatives, Fmoc-Phe-DAP (**1**), Fmoc-3F-Phe-DAP (**2**), and Fmoc-F_5-Phe-DAP (**3**) (**Figure 1**), upon addition of varying amounts of glutamate and aspartate salts. We discovered that these anionic amino acids influence both the morphology of the resulting assemblies as well as the properties of these assemblies. Interestingly, only Fmoc-3F-Phe-DAP (**2**)/glutamate mixtures formed stable, self-supporting hydrogels. Mixtures of glutamate with Fmoc-Phe-DAP (**1**) and Fmoc-F_5-Phe-DAP (**3**) underwent self-assembly, but the resulting solution assemblies failed to form strong hydrogel networks. In contrast, mixtures of aspartate with all Fmoc-Phe-DAP derivatives self-assembled into weak hydrogel networks that quickly precipitated within 30 minutes. These studies demonstrate that hybrid supramolecular amino acid materials elicit unique emergent properties relative to materials derived from the individual components. Further, these results invite further study to determine the mechanistic basis for these unique properties and to characterize the biochemical properties of these hydrogels for drug delivery and tissue engineering applications.

2. MATERIALS AND METHODS

Materials. Fmoc protected amino acids, monosodium amino acids and organic solvents were purchased commercially and used without further purification. Compounds **1**−**3** were synthesized in accordance with previously reported protocols.[40] Water used for self-assembly and hydrogelation studies was purified using a nanopure filtration system (Barnstead NANOpure, 0.2 μm filter, 18.2 MΩ cm).

Self-Assembly Conditions. All self-assembly experiments were prepared at a total volume of 1 mL and with a final Fmoc-Phe-DAP derivative (compound **1**, **2**, or **3**) concentration of 15 mM. Stock solutions (500 mM) of the monosodium salts of glutamic acid and aspartic acid were used to create mixtures with compounds **1**–**3**. Briefly, compounds **1**–**3** (0.21 mmol) were each dissolved in 7 mL of water and heated to 80 °C to obtain 30 mM stock solutions of compounds **1**–**3**. The volume of these solutions was adjusted with varying amounts of water (see **Table S1**) prior to the addition of anionic amino acids in order to ensure the final volume of each mixture was 1 mL. Self-assembly was initiated by the addition of 30 μL of the stock solutions of either glutamic acid or aspartic acid to 0.5 mL of the solutions of Fmoc-Phe-DAP-derived compounds **1**–**3**. Self-assembly of compounds **1**–**3** (15 mM) was evaluated at varying concentrations of aspartate and glutamate, including 15 mM (1 equivalent relative to Fmoc-Phe-DAP derivative), 30 mM (2 equivalents), 45 mM (3 equivalents), 60 mM (4 equivalents), 75 mM (5 equivalents), 90 mM (6 equivalents), 105 mM (7 equivalents), 120 mM (8 equivalents), 135 mM (9 equivalents), and 150 mM (10 equivalents). Upon addition of aspartate or glutamate salts to compounds **1**–**3**, each solution was briefly agitated using a vortex mixer and the mixtures were allowed to stand at room temperature for 30 minutes. Hydrogel formation was confirmed when the resulting mixtures did not flow upon vial inversion. Detailed procedures for preparing the assemblies are summarized in **Table S1** (Supporting Information).

Of compounds **1**–**3**, only Fmoc-3F-Phe (**2**) was found to form stable hydrogel networks in the presence of glutamate or aspartate salts. Accordingly, comparison hydrogels of compounds **2** were prepared by the addition of NaCl to solutions of **2**, consistent with our prior reports for self-assembly and hydrogelation of these compounds.[40] Fmoc-3F-Phe (**2**)/NaCl hydrogels for this study were prepared at 15 mM concentrations of **2** and 114 mM NaCl (7.6 equivalents with respect to compound **2**). To prepare these hydrogels, compound **2** was dissolved in 0.8 mL of water with heating. Gelation was triggered by addition of 0.2 mL of a 570 mM NaCl solution followed by brief agitation of the solution using a vortex mixer. Hydrogelation was observed within one minute.

Transmission Electron Microscopy. Transmission electron microscopy (TEM) images of the assemblies were obtained using a Hitachi 7650 transmission electron microscope with an accelerating voltage of 80 kV. Aliquots of assembled materials (5 μL) were applied directly onto 200 mesh carbon-coated copper grids and allowed to stand for 2 minutes. Remaining liquid was carefully removed by capillary action using filter paper. This was followed by addition of a second 5 μL aliquot of the material and the grid was again allowed to stand for 2 minutes. The remaining liquid was removed, and the grids were then stained with 2% (*w/v*) uranyl acetate (5 μL) for 2 minutes. Remaining stain solution was again removed by capillary action, and the grids were allowed to air-dry for 10−15 minutes. TEM images of each assembly was recorded at 4 hours, 24 hours, and 1 week after initiation of self-assembly. Dimensions of the nanostructures were determined using ImageJ software and are reported as the average of at least 100 independent measurements with error reported as the standard deviation value.

Oscillatory Rheology. Rheological measurements were performed using a TA Instruments Discovery HR-2 rheometer. A 20 mM parallel plate geometry was used for the experiments. To

perform the rheological experiments, hydrogels at a final volume of 1 mL were prepared in a 1.5 mL microcentrifuge tube. Deposition of the hydrogel onto the rheometer plate was performed by cutting the centrifuge tube at the 0.5 mL line using a razor blade and the cylindrical hydrogel was placed directly onto the Peltier plate by gently pushing it out of the bottom of the tube from the top. The gap for each individual experiment was adjusted to 1 mm. Strain sweep experiments were performed first to determine the linear viscoelastic region for each hydrogel. Strain sweep measurements were performed from 0.01−100% strain at a constant frequency of 6.283 rad s^{-1}. Next, frequency sweep experiments were performed at a constant strain within the linear viscoelastic region. The frequency sweep experiments for each sample were performed from 0.1−100 rad s^{-1} at a constant strain of 0.2%, which falls within the linear viscoelastic region for all the hydrogels. Values at the upper end of the frequency sweep experiments were eliminated for all the data points for which the raw phase angle increased above 175° as recommended for the TA DHR series of rheometers. The values beyond this point are dominated by the instrument inertial torque instead of the sample torque[41]. The reported values for storage and loss moduli (G′ and G″, respectively) are the average of five distinct measurements on separate hydrogels and all five associated measurements are shown on the associated plots. Finally, the average G′ values were used to calculate the mesh size of the hydrogels according to **equation 1** below where ξ is the mesh size, k_B is the Boltzman constant, and T is temperature.[50, 51]

$$\xi = \left(\frac{G'}{k_{\boldsymbol{B}}\, T}\right)^{-\frac{1}{3}}$$

Equation 1

3. RESULTS AND DISCUSSION

Multicomponent assembly of Fmoc-Phe-DAP derivatives and anionic amino acids. We have previously demonstrated that Fmoc-Phe-DAP derivatives, including Fmoc-Phe-DAP (**1**), Fmoc-3F-Phe-DAP (**2**), and Fmoc-F_5-Phe-DAP (**3**) (**Figure 1**), undergo effective self-assembly into hydrogels that have the appropriate emergent properties for functional drug delivery.[43, 52] These compounds are soluble in water due to the positively charged ammonium cation of the C-terminal diaminopropane group. However, these cationic compounds do not form self-supporting supramolecular hydrogels without solution screening counterions that reduce charge repulsion between the ammonium groups. Compounds **1**–**3** spontaneously form hydrogel networks in presence of NaCl (114 mM) as an initiating agent.[40]Further, we have also examined the variations in the properties of these self-assembled materials in the presence of different inorganic salts as counterions.[42] The nature of the screening counterion can direct the self-assembly of Fmoc-Phe-DAP derivatives into a broad range supramolecular architectures, including nanotubes, fibrils, and nanosheets of various dimensions and morphologies. These various assemblies in turn have a range of emergent properties, with some forming stable hydrogel networks, while others form precipitates or colloidal suspensions. The sensitivity of these Fmoc-Phe-DAP derivatives to the environment to tune supramolecular properties provides interesting opportunities for the development of novel hybrid biomaterials composed of Fmoc-Phe-DAP derivatives mixed with other agents with complementary properties.

Based on the observation that the solvent counterions dramatically affect the self-assembly of compounds **1**–**3**, we initiated a study to explore a multicomponent approach to develop hybrid hydrogels composed of charge complementary amino acids, cationic Fmoc-Phe-DAP derivatives

and anionic amino acids. Specifically, we have studied the assembly behavior and emergent properties of a series of Fmoc-Phe-DAP derivatives, compounds **1**–**3**, in the presence of anionic monosodium glutamate acid and monosodium aspartic acid. We hypothesized that the negative charge of glutamate and aspartate would provide complementary interactions with Fmoc-Phe-DAP derivatives that would enable effective assembly. We also hypothesized that the complementary charge interactions would give rise to Fmoc-Phe-DAP assemblies with unique properties relative to the hydrogels that are formed from these amino acids in the presence of inorganic salts, including NaCl. We interrogated these hypotheses by characterizing the assembly of compounds 1–3 in the presence of varying amounts of monosodium glutamate and monosodium aspartate. We first determined if any of these mixtures resulting in self-supporting hydrogel networks. Next, we examined the resulting morphology of the resulting assemblies using transmission electron microscopy imaging. Finally, we characterized the emergent viscoelasticity for mixtures that formed hydrogels compared to our previously reported hydrogels of these compounds formed in the presence of NaCl.

Multicomponent assembly of compounds **1**–**3** with glutamate or aspartate was explored in simple aqueous solutions without other explicitly added materials. Compounds **1**–**3** were dissolved in water by heating followed by sonication, followed by addition of aqueous solutions of anionic amino acids to promote self-assembly. The concentration of compounds **1**–**3** was maintained at 15 mM for these studies and the concentration of the anionic amino acids was varied from 1 equivalent (15 mM) to 10 equivalents (150 mM) with respect to the Fmoc-Phe-DAP derivatives. All hydrogels had pH values ranging from 6.6-7. Interestingly, the assemblies formed by these various mixtures was sensitive to both the structure of the cationic Fmoc-Phe-DAP derivative and to the specific anionic partner, glutamate or aspartate.

First, we found that compounds **1**–**3** exhibited different assembly and gelation behavior in the presence of glutamate ions **(Figure 2)**. At lower concentrations of glutamate ions (15 mM and 30 mM glutamate), compounds **1** and **2** (15 mM) failed to form self-supporting hydrogels (**Figure 2A** and **2B**). The mixtures of compound **1** and glutamate formed suspensions/precipitates at 1 and 2 equivalents of glutamate while the mixtures of compound **2** and glutamate at the same glutamate concentrations were transparent solutions. Upon increasing the concentration of glutamate ions to 3 equivalents (45 mM), mixtures compounds **1** and **2** with glutamate formed self-supporting hydrogels (**Figure 2A** and **2B**) as indicated by resistance to flow of these materials upon vial inversion. Mixtures of compounds **1** and **2** with 3–10 equivalents of glutamate all formed self-supporting hydrogels. The hydrogels of compound **1** with glutamate developed a cloudy appearance over 24 hours while the hydrogels of compound **2** with glutamate remained transparent over 24 hours. These observations are consistent with our previous reports in which the fluorination of the benzyl side chain of Fmoc-3F-Phe-DAP (**2**) provides enhanced self-assembly and hydrogelation capacity relative to the parent Fmoc-Phe-DAP (**1**) derivative.[40]

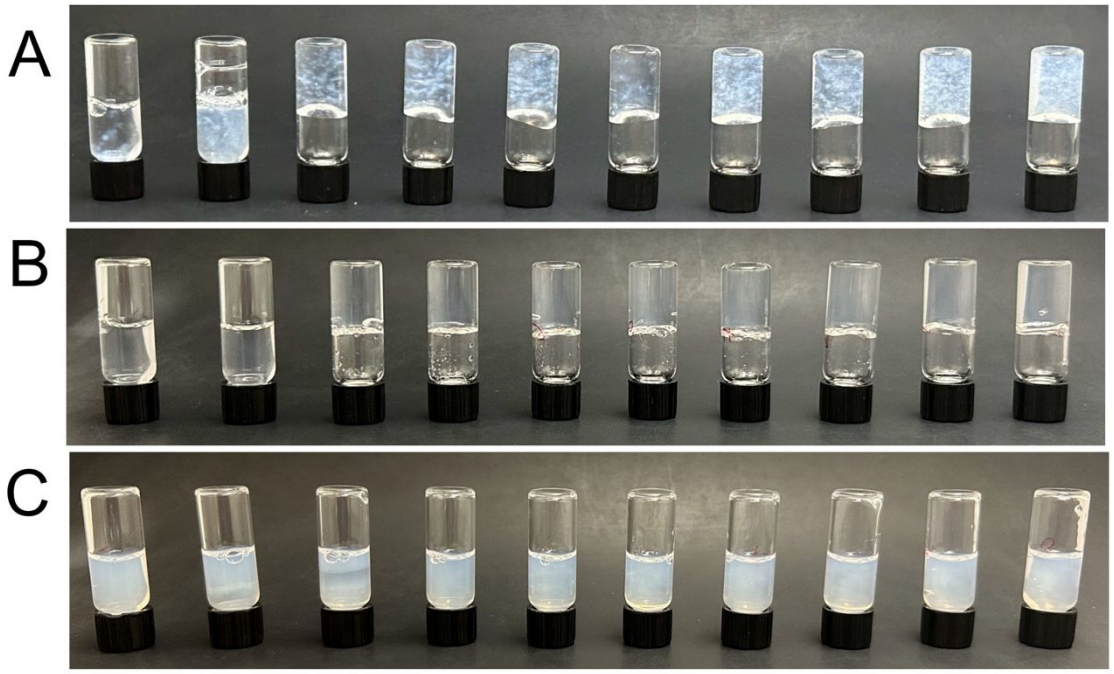

Figure 2. Digital images of assemblies of Fmoc-Phe-DAP derivatives 24 hours after addition of glutamate. Assemblies are composed of 15 mM Fmoc-Phe-DAP derivative with 1–10 equivalents of glutamate (1 equivalent of glutamate to 10 equivalents of glutamate from left to right, respectively). **A.** Compound **1**/glutamate, **B.** Compound **2**/glutamate, **C.** Compound **3**/glutamate.

Interestingly, the perfluorinated Fmoc-F_5-Phe-DAP derivative, compound **3**, fails to form self-supporting hydrogels at any of the concentrations of glutamate ions studied up to 10 equivalents of glutamate relative to **3** (**Figure 2C**). All the **3**/glutamate mixtures, from 1–10 equivalents of glutamate, instead formed colloidal suspensions. Prior studies of compound **3** have often shown that this derivative has superior gelation capacity relative to compounds **1** and **2** upon addition of NaCl.[40, 42] Thus, it was unexpected that compound **3** would fail entirely to form hydrogels when mixed with glutamate. The appearance of these solutions as colloidal suspensions upon addition of glutamate to solutions of **3** is suggestive of supramolecular assembly, although the reasons that

these assemblies do not entangle into hydrogel-forming networks was not apparent. Some insight was gained by characterizing the morphology of these assemblies using TEM imaging as described in the following section.

Next, we found that the assembly behavior of compounds **1**–**3** varied dramatically when aspartate was used as an initiating agent instead of glutamate (**Figure 3**). Compound **1** rapidly forms precipitates upon the addition of aspartate even at only 1 equivalent of added aspartate (**Figure 3A**). In contrast, compound **2** forms self-supporting hydrogels in the presence of aspartate ions, although these hydrogels are stable only for a very brief period; the assemblies of compound **2** with aspartate begin to precipitate within 30 minutes (**Figure 3B**). An example of the progression of precipitate formation in mixtures of compound **2** and aspartate (7 equivalents) is shown in **Figure S1** (Supporting Information). The formation of precipitates in hydrogels of compound 2 with aspartate increases with time; after 12 hours, these assemblies completely precipitate and the hydrogel network is disrupted. As with the glutamate mixtures, mixtures of compound **3** with aspartate exhibited unique assembly behavior compared with the aspartate mixtures of compounds **1** and **2**. Solutions of compound **3** formed turbid colloidal suspensions upon addition of aspartate (**Figure 3C**). At final aspartate concentrations of 5 equivalents or higher, compound **3** was observed to form weak, partial hydrogels that were not highly stable to mechanical disruption.

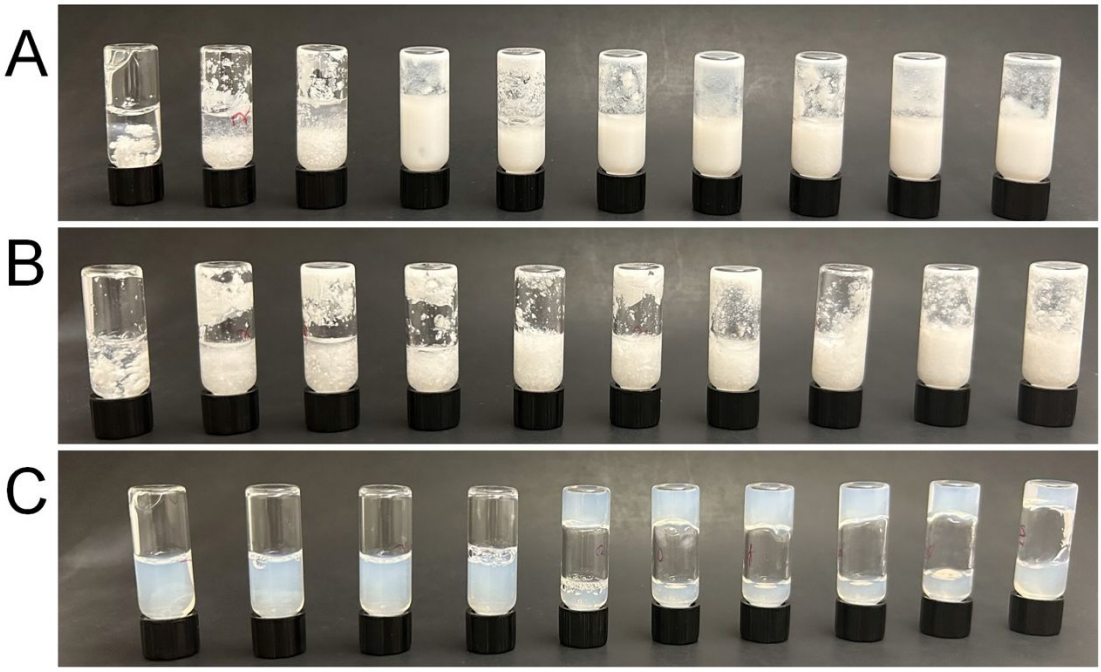

Figure 3. Digital images of assemblies of Fmoc-Phe-DAP derivatives 24 hours after addition of aspartate. Assemblies are composed of 15 mM Fmoc-Phe-DAP derivative with 1–10 equivalents of aspartate (1 equivalent of asparate to 10 equivalents of aspartate from left to right, respectively). **A.** Compound **1**/aspartate, **B.** Compound **2/** aspartate, **C.** Compound **3**/ aspartate.

Morphological properties of multicomponent hydrogels of Fmoc Phe-DAP derivatives. Transmission electron microscopy (TEM) was used to characterize the morphology of the assemblies formed from mixtures of compounds **1**, **2**, and **3** with glutamate and aspartate. TEM images were recorded after 4 hours, 24 hours, and 7 days of initiation of assembly by addition of anionic amino acids. Representative TEM images were obtained from mixtures containing 7 equivalents of anionic amino acid relative to Fmoc-Phe-DAP derivatives **1**, **2**, or **3** (15 mM). We also evaluated the morphological properties of assemblies of compounds **1**–**3** in the presence of NaCl (114 mM, 7.6 equivalents of chloride ions) as a comparison of our previously reported

assemblies of these derivatives to those formed from mixtures with glutamate and aspartate. TEM images of these mixtures reveal unique assembly morphologies in the presence of NaCl, glutamate, or aspartate screening partners. It should be noted that all TEM images were obtained under conditions where the samples were dried during the sample deposition process. As such, some of the observed morphologies may be subject to drying artifacts, particularly assemblies that have nanotube morphologies.

The TEM images of assemblies of compound **1** under these various conditions show unique features as a function of assembly partner (**Figure 4A** and **4B**, **Figure S2**). Fmoc-Phe-DAP (**1**) formed various morphological structures in presence of NaCl. Consistent with our previous reports,[40] upon addition of NaCl, compound **1** self-assembled to form twisted nanoribbons that ranged from 30–90 nm wide with some ribbons as wide as 200–300 nm also observed (**Figure S2A**). After 24 h, these nanotube structures of average width 319 ± 80 nm begin to appear along with the twisted nanoribbons (**Figure S2B**). Over 7 days, the sheets twist further and entangle to form mature nanotubes of diameter up to 500 nm (**Figure S5A**, Supporting Information). In contrast, in the presence of glutamate ions, compound **1** forms an entangled network of thin twisted nanoribbons 40 ± 14 nm wide (**Figure S2C**). No significant changes in the assembly morphology were observed for the assembly of compound **1** in the presence of glutamate ions over a period of 24 hours (**Figure 4A**, **Figure S2D**). Twisted ribbons remain as the dominant morphology for compound **1**/glutamate mixtures even after 7 days (**Figure S5B**, Supporting Information). Mixtures of compound **1** with aspartate rapidly form nanotubes within a few hours of addition of glutamate (**Figure S2E** and **S2F**). These nanotubes are highly polymorphic and vary in diameter from 172 nm to 695 nm. After 7 days, even larger nanotubes with diameters up to 1 μm are also observed (**Figure 4B**, **Figure S5C**).

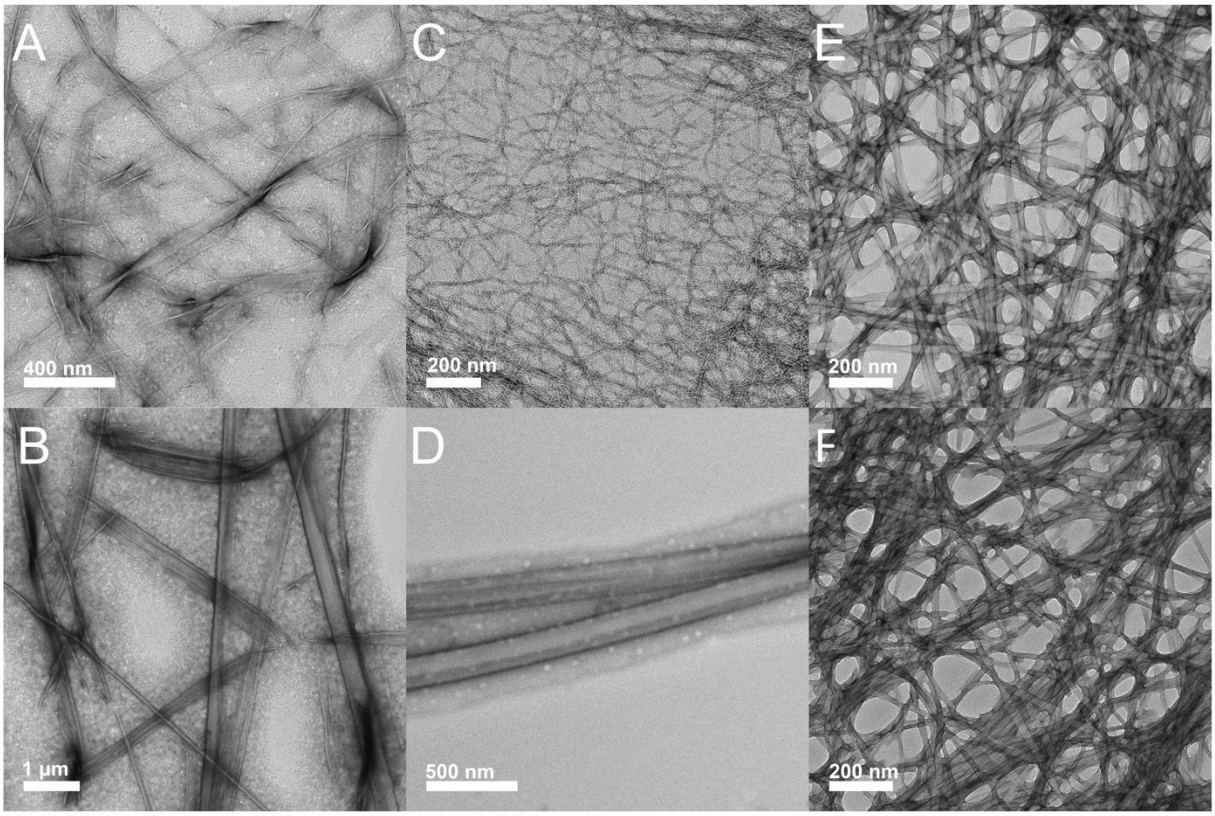

Figure 4. TEM images of Fmoc-Phe-DAP (**1**), Fmoc-3F-Phe-DAP (**2**), and Fmoc-F_5-Phe-DAP (**3**) (15 mM) with glutamate (7 equivalents) or asparate (7 equivalents) after 24 hours of assembly. **A.** Fmoc-Phe-DAP (**1**)/glutamate after 24 hours, **B.** Fmoc-Phe-DAP (**1**)/aspartate after 24 hours, **C.** Fmoc-3F-Phe-DAP (**2**)/glutamate after 4 hours, **D.** Fmoc-3F-Phe-DAP (**2**)/aspartate after 24 hours, **E.** Fmoc-F_5-Phe-DAP (**3**)/glutamate after 4 hours, **F.** Fmoc-F_5-Phe-DAP (**3**)/aspartate after 24 hours.

TEM images of assemblies of compound **2** in the presence of NaCl, glutamate, and aspartate also showed that assembly of compound **2** is sensitive to the added counterion partner (**Figure 4C** and **4D**, **Figure S3**). In the presence of NaCl, formation of a dense network of nanofibers of average diameter 7.3 ± 4.2 nm is observed after 4 hours of addition of NaCl (**Figure S3A**). These nanofibers further assemble over 24 hours to form twisted bundles of fibrils. The average width of

these bundles was found to be 16.4 ± 7.3 nm (**Figure S3B**). The formation of nanofibers is also observed in the presence of glutamate ions. However, these fibers are much narrower in diameter with an average diameter of 4.8 ± 1.8 nm. In contrast to the fibers formed by **2** with NaCl, the **2**/glutamate fibers do not entangle to form bundles of fibrils over time (**Figure 4C**, **Figure S3C** and **S3D**). A similar nanofibrous network is observed over a period of 7 days with no significant change in the morphology (**Figure S5E**, Supporting Information). The presence of aspartate significantly alters the morphological features of the assemblies of compound **2.** As stated above, self-assembly of compound **2** in the presence of counterions generally results in nanofibrous morphology. However, in the presence of aspartate a range of polymorphic structures are observed for compound **2**. Nanotubes that vary in diameter from 100 nm to 2 μm are observed within 4 hours of addition of aspartate to compound **2** (**Figure S3E**) and these persist after 24 hours (**Figure 4D** and **Figure S3F**). Along with these nanotube structures, thin fibers of average width 7.5 ± 2.4 nm in diameter are also observed (**Figure S6**, Supporting Information), although nanotubes are by far the more dominant morphology. In addition, over a period of 7 days, no significant change in morphology is observed (**Figure S5F**, Supporting Information).

Fmoc-F_5-Phe-DAP (**3**) has been previously shown to form self-supporting hydrogels in the presence of NaCl (114 mM).[34, 40] In the presence of NaCl, compound **3** self-assembles to form nanofibers 13.0 ± 4.6 nm in diameter at 15 mM concentrations of **3** (**Figure S4A** and **S4B**). The morphological features remain unaffected over a period of 7 days (**Figure S5G**, Supporting Information). Interestingly, herein we have demonstrated that compound **3** fails to form self-supporting hydrogels in the presence of anionic amino acids, even up to 10 molar equivalents of anionic amino acid. TEM images reveal that mixtures of compound **3** with glutamate or aspartate show distinct assembly features. Although a self-supporting hydrogel is not formed in presence of

glutamate or aspartate ions, a nanofibrous morphology is observed for the assemblies of compound **3** 4 hours after addition of glutamate that remain unchanged over 24 hours (**Figure 4E**, **Figure S4C** and **S4D**). The average width of the fibers in mixtures of **3** and glutamate is 14 ± 4 nm. Similar fibers 17 ± 5 nm in diameter are formed in mixtures of compound **3** and aspartate (**Figure 4F**, **Figure S4E** and **S4F**). After 7 days, the fibers of **3**/glutamate and **3**/aspartate mixtures maintain similar morphologies (**Figure S5H** and **S5I**, Supporting Information).

Viscoelastic properties of multicomponent hydrogels. The Fmoc-Phe-DAP derivatives **1** and **2** formed self-supporting hydrogels stable for long time periods in the presence of glutamate ions. Therefore, we performed oscillatory rheology experiments to evaluate the viscoelastic properties of these hydrogels. All experiments were performed 24 hours after initiation of gelation. Frequency sweep experiments were performed at a constant strain of 0.2%, which falls within the linear viscoelastic region of the hydrogels as evident from initially performed amplitude sweep experiments (**Figure S7** and **S8**, Supporting Information). Frequency sweep experiments provided values for the viscoelastic storage (G') and loss (G") moduli, which are reported herein from the average of five frequency sweep experiments for each hydrogel. Error is reported as the standard deviation of these averages.

Representative rheological characterization experiments were performed using hydrogels with a final glutamate concentration of 105 mM (7 equivalents relative to the Fmoc-Phe-DAP derivative, which was at 15 mM). This concentration of glutamate ions was chosen because is it comparable to the concentration of chloride ions of our previously reported hydrogels (114 mM NaCl). The G' value was greater than G" for all the evaluated hydrogels of mixtures of compounds **1** and **2** with glutamate. The G' value for hydrogels of compound **1**/glutamate mixtures was lower

than 100 Pa (**Figure S9**, Supporting Information). Thus, compound **1**/glutamate hydrogels are viscoelastically quite weak. Similarly, hydrogels of compound **1** formed with NaCl have also been previously shown to be weak relative to hydrogels of compounds **2** and **3** with NaCl.[40] Here, we again found that Fmoc-Phe-DAP (**1**)/NaCl hydrogels were stable only for a short time, forming precipitates within 24 h. These hydrogels did not retain water when placed on the Peltier plate; rheological measurements were therefore not performed for these hydrogels.

In contrast, hydrogels of Fmoc-3F-Phe-DAP (**2**)/glutamate mixtures were found to be stable. The storage moduli of these hydrogels are significantly higher than the hydrogels of compound **1**/glutamate formulated under identical conditions. We characterized the viscoelasticity of compound **2**/glutamate hydrogels at a constant concentration of compound **2** (15 mM) and a range of glutamate concentrations, including 45 mM (3 molar equivalents relative to **2**), 75 mM (5 equivalents), 105 mM (7 equivalents), and 135 mM (9 equivalents). These hydrogels were compared a hydrogel of compound 2 (15 mM) with 115 mM NaCl, which were found to have an average G' value of 7414.34 ± 425.3 Pa and a G" value of 1372.29 ±170.6 Pa (**Figure 5A**). The hydrogels of compound **2**/glutamate were found to increase in viscoelasticity as a function of increasing glutamate concentrations (**Table 1**). At lower glutamate concentrations of 45 mM (3 equivalents relative to compound **2**), the storage moduli of these hydrogels are lower than 100 Pa (**Figure S10**, Supporting Information). Upon increasing the concentration of glutamate to 5–9 molar equivalents relative to **2**, an upward trend is observed for the storage moduli of these hydrogels (**Figure 5**, **Table 1**). The average G' value for hydrogels of compound **2**/glutamate (15 mM **2**, 75 mM (5 equivalents) glutamate) were 209 ± 43 Pa (**Figure 5B**). The average G' value for hydrogels of compound **2**/glutamate (15 mM **2**, 105 mM (7 equivalents) glutamate) were 770 ±

105 Pa (**Figure 5C**). Finally, the average G' value for hydrogels of compound **2**/glutamate (15 mM **2**, 135 mM (9 equivalents) glutamate) were 2000 ± 173 Pa (**Figure 5D**). Thus, increasing glutamate concentrations served to strengthen the viscoelasticity of these multicomponent hydrogels.

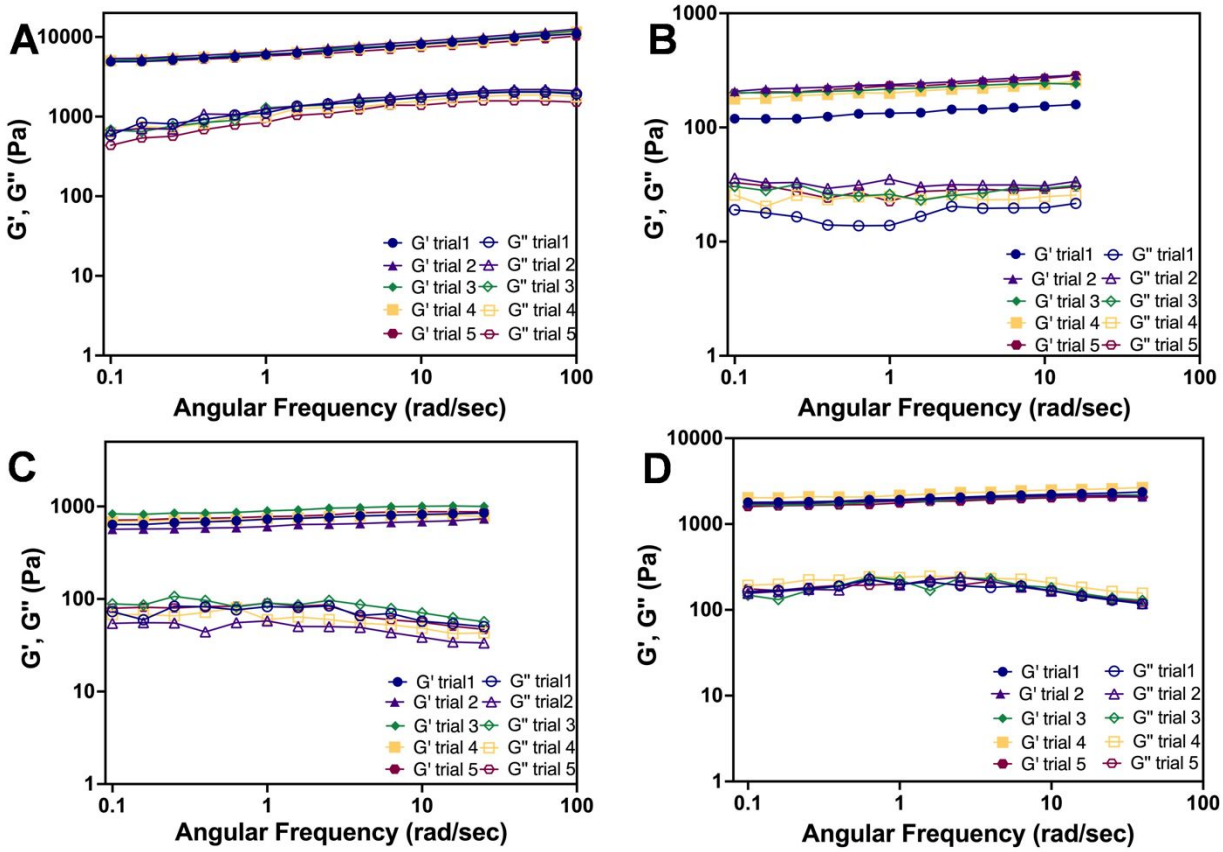

Figure 5. Comparative oscillatory rheology frequency sweep viscoelasticity data for Fmoc-3F-Phe-DAP (**2**)/NaCl (15 mM compound **2**, 114 mM NaCl) and Fmoc-3F-Phe-DAP (**2**)/glutamate (15 mM compound **2**, varying glutamate concentrations) hydrogels. **A.** Fmoc-3F-Phe-DAP (**2**)/NaCl, **B.** Fmoc-3F-Phe-DAP (**2**)/5 equivalents glutamate, **C.** Fmoc-3F-Phe-DAP (**2**)/7 equivalents glutamate, **D.** Fmoc-3F-Phe-DAP (**2**)/9 equivalents glutamate.

Table 1. Oscillatory rheology frequency sweep evaluation of storage modulus (G′), loss modulus (G″), and average hydrogel mesh size for hydrogels of Fmoc-3F-Phe-DAP (**2**)/glutamate mixtures. Rheology experiments were performed on hydrogels with a constant concentration of compound **2** (15 mM) and concentrations of glutamate at 3, 5, 7, and 9 molar equivalents.

Glutamate concentration (mM)	**G′ (Pa)**	**G″ (Pa)**	**Mesh size (nm)**
45 (3 equivalents)	21 ± 5	8 ± 2	58
75 (5 equivalents)	209 ± 43	26 ± 5	27
105 (7 equivalents)	770 ± 105	67 ± 14	18
135 (9 equivalents)	2000 ± 173	186 ± 16	13

We also calculated the approximate mesh size of the Fmoc-3F-Phe-DAP (**2**)/glutamate hydrogels using the storage moduli values using **equation 1** (see Materials and Methods). The mesh size, an inherent property of nanofibrous networks, is an important parameter that influences the potential of these materials to be used for biological applications like drug delivery, where the mesh size in part determines diffusion parameters of materials through the hydrogel. **Table 1** summarizes the calculated mesh size of the hydrogels of compound **2** in presence of glutamate. In For comparison, the calculated mesh size of Fmoc-3F-Phe-DAP (**2**) hydrogels with 114 mM NaCl is 8.2 nm. A decrease in the mesh size is observed upon increasing the concentration of glutamate ions. Further, a clear variation is observed between the mesh size of the hydrogels in presence of glutamate and chloride as screening molecules. It is evident from our rheological experiments that the multicomponent approach to design novel hybrid hydrogels results in the development of materials with tunable properties. Such materials with unique and tunable properties have potential

as useful self-assembled systems for various biological applications that include drug delivery and tissue engineering.

Discussion. These studies provide interesting insights into the influence of anionic amino acids on the assembly of cationic Fmoc-Phe-DAP derivatives. First, it is interesting that the assembly morphologies of both Fmoc-Phe-DAP (**1**) and Fmoc-3F-Phe-DAP (**2**) are so highly sensitive to counterion identity, while the assembly morphology of Fmoc-F_5-Phe-DAP (**3**) is seemingly unaffected by the counterion. For example, Fmoc-3F-Phe-DAP (**2**) forms thin fibers in the presence of both NaCl and glutamate. Strikingly, when aspartate is added as a counterion, the resulting Fmoc-3F-Phe-DAP (**2**) mixtures form markedly different nanotube structures. In contrast, Fmoc-F_5-Phe-DAP (**3**) forms thin fibers of similar morphology regardless of the counterion partner. This is consistent with our prior work in which Fmoc-F_5-Phe-DAP (**3**) assembly morphology was likewise insensitive to the identity of inorganic counterion salts that otherwise had a significant impact on the morphology of assemblies of compounds **1** and **2**. This observation strengthens the case that the perfluorinated benzyl ring of Fmoc-F_5-Phe-DAP (**3**) plays a dominant directing role in the self-assembly of this derivative that overcomes environmental effects on assembly pathways. Fmoc-F_5-Phe-DAP (**3**) is significantly more hydrophobic than either Fmoc-Phe-DAP (**1**) or Fmoc-3F-Phe-DAP (**2**), which may play a role in the differing self-assembly properties. The dramatically different electronics of the highly electron-deficient benzyl side chain of Fmoc-F_5-Phe-DAP (**3**) may also play a significant role in these effects.

In this study, the only the Fmoc-3F-Phe-DAP (**2**)/glutamate mixtures formed stable, self-supporting hydrogel networks. The fact that these assemblies were all found to be thin, highly entangled fibers is consistent with a material that effectively forms a network that elicits emergent viscoelastic gelation. The ribbon, sheet, and nanotube morphologies observed with mixtures of

Fmoc-Phe-DAP (**1**) and the aspartate mixtures with both Fmoc-Phe-DAP (**1**) and Fmoc-3F-Phe-DAP (**2**) appear to be less efficient at forming entangled networks resulting in hydrogelation. The larger dimension of these types of assemblies is consistent with this reasoning, as is the observation that these assemblies tend to be prone to lower solubility or even precipitation, which complicates establishment of hydrogel networks. However, based on this reasoning it is curious that the various mixtures of Fmoc-F_5-Phe-DAP (**3**) with glutamate and aspartate, which are all fibrous assemblies do not form stable hydrogel networks (although the Fmoc-F_5-Phe-DAP (**3**)/aspartate mixtures were weakly viscoelastic at the higher concentrations of aspartate, these mixtures were not self-supporting upon mechanical agitation).

These observations raise interesting questions about the relationships between assembly morphology and emergent hydrogel network formation. The simplifying assumption is that materials that form flexible, fibrous assemblies will most effectively form hydrogel network. Materials that form larger, non-fibrous assemblies (including nanosheets and nanotubes) will less effectively form entangled networks. Why then do the Fmoc-F_5-Phe-DAP (**3**)/aspartate or glutamate mixtures, which appear to be thin, relatively flexible fibrous assemblies, not also form hydrogels? We posit a few hypothetical possibilities. First, the fibers formed in the hydrogels of Fmoc-3F-Phe-DAP (**2**) mixed with glutamate are <10 nm in diameter, whereas the fibers formed by Fmoc-F_5-Phe-DAP (**3**) with glutamate are 14–18 nm in diameter and appear less flexible than the Fmoc-3F-Phe-DAP (**2**) counterparts. These subtle morphological differences may be sufficient to alter the network to such an extent that explain the variance in emergent viscoelastic properties between the two materials. Second, the greater hydrophobicity of the Fmoc-F_5-Phe-DAP (**3**) materials relative to the Fmoc-3F-Phe-DAP (**2**) assemblies is likely to have a significant impact on the interactions of these materials with water, making the network of the Fmoc-F_5-Phe-DAP

(**3**) mixtures less able to immobilize water within the network. Finally, perhaps the dramatically different electronic properties of Fmoc-F_5-Phe-DAP (**3**) facilitate anion-π interactions with the partner glutamate or aspartate amino acids that result in surface passivation of these amino acids on the assemblies to an extent that fiber-fiber interactions that mediate the entangled networks are impeded. These various possibilities invite exciting possibilities for future study to gain additional insight into the mechanistic basis by which the constituents of these multicomponent materials interact to influence both assembly and emergent assembly properties.

Finally, there are additional unanswered questions raised by these studies. Why do aspartate and glutamate exert such different effects on the assembly and emergent properties of these mixtures? How are glutamate and aspartate incorporated into the assemblies and resulting networks? Are they interspersed within the packing structure of the assemblies with the Fmoc-Phe-DAP derivatives or are they playing a surface role, primarily interacting with the cationic surface of self-assembled Fmoc-Phe-DAP derivative assemblies? These questions invite additional future interrogation of these and related systems to gain deeper fundamental understanding of the interactions between the cationic and anionic components of these materials and how these interactions influence the properties of the assemblies.

4. CONCLUSION

Herein we have reported novel multicomponent supramolecular materials composed of cationic Fmoc-Phe-DAP derivatives and complementary anionic amino acids, aspartate and glutamate. These mixtures form assemblies that are sensitive to the structure of the Fmoc-Phe-DAP derivative and to the structure of the anion amino acid. The matrix of possible combinations that arise from the various combinations of the three cationic Fmoc-Phe-DAP derivatives and the two anionic amino acids result in a variety of observed assemblies, including nanofibers, nanoribbons, and

nanotubes. Further, these various assemblies exhibit a range of emergent materials properties, including hydrogel viscoelasticity, colloidal suspension, and precipitated supramolecular scaffolds. These studies illustrate the versatility that combining even small sets of supramolecular building can provide in the development of novel biomaterials and invite further study to define the mechanistic basis and functional scope of these and related materials.

DATA AVAILABILITY

TEM and additional oscillatory rheology data are available in the Electronic Supplemental Information file (Supporting Information). Data from oscillatory rheology experimental results presented in Figure 5A, Figure 5B, Figure 5C, Figure 5D, Figure S7A (Supporting Information), Figure S7B (Supporting Information), Figure S8 (Supporting Information), Figure S9 (Supporting Information), Figure S10 (Supporting Information) are included in a second supplemental spreadsheet file entitled “Ghosh Rheology Data 2024.”

CONFLICTS OF INTEREST

The authors declare no conflicts of interest.

ACKNOWLEDGEMENTS

This work was supported by the U.S. Department of Defense (US Army Medical Research Acquisition Activity, W81XWH-20-1-0112) and the National Science Foundation (U.S. National Science Foundation Convergence Accelerator, Grant ITE-2344389; Division of Chemistry, Grant CHE-2304852). We thank Karen Bentley at the URMC Electron Microscope Shared Resource for her assistance in TEM imaging experiments.

REFERENCES

1. S. J. Buwalda, T. Vermonden and W. E. Hennink, *Biomacromolecules*, 2017, **18**, 316-330.
2. S. Bianco, M. Hasan, A. Ahmad, S.-J. Richards, B. Dietrich, M. Wallace, Q. Tang, A. J. Smith, M. I. Gibson and D. J. Adams, *Nature*, 2024, **631**, 544-548.
3. C. C. Piras and D. K. Smith, *J. Mater. Chem. B*, 2020, **8**, 8171-8188.
4. J. F. Delgado, W. F. Pritchard, N. Varble, T. L. Lopez-Silva, A. Arrichiello, A. S. Mikhail, R. Morhard, T. Ray, M. M. Havakuk, A. Nguyen, T. Borde, J. W. Owen, J. P. Schneider, J. W. Karanian and B. J. Wood, *Sci Rep*, 2024, **14**, 13352.
5. J. Cai, J. Guo and S. Wang, *Gels*, 2023, **9**, 98.
6. J. Gamboa, S. Paulo-Mirasol, F. Estrany and J. Torras, *ACS Appl. Bio Mater.*, 2023, **6**, 1720-1741.
7. M. M. El Sayed, *J Polym Environ*, 2023, **31**, 2855-2879.
8. N. H. Thang, T. B. Chien and D. X. Cuong, *Gels*, 2023, **9**, 523.
9. Y. Li, F. Wang and H. Cui, *Bioeng. Transl. Med.,* 2016, **1**, 306-322.
10. M. Nambiar and J. P. Schneider, *J. Pept. Sci.*, 2022, **28**, e3377.
11. V. Leyva-Aranda, S. Singh, M. J. Telesforo, S. Young, C. Yee and J. D. Hartgerink, *ACS Biomater. Sci. Eng.*, 2024, **10**, 1448-1460.
12. M. A. Elsawy, J. K. Wychowaniec, L. A. Castillo Díaz, A. M. Smith, A. F. Miller and A. Saiani, *Biomacromolecules*, 2022, **23**, 2624-2634.
13. M. M. Harper, M. L. Connolly, L. Goldie, E. J. Irvine, J. E. Shaw, V. Jayawarna, S. M. Richardson, M. J. Dalby, D. Lightbody and R. V. Ulijn, in *Peptide Self-Assembly: Methods and Protocols*, eds. B. L. Nilsson and T. M. Doran, Springer New York, New York, NY, 2018, DOI: 10.1007/978-1-4939-7811-3_18, pp. 283-303.
14. D. Marin and S. Marchesan, *Nanomaterials*, 2022, **12**, 2147.
15. S. R. Caliari and J. A. Burdick, *Nat. Methods*, 2016, **13**, 405-414.
16. M. J. Sis and M. J. Webber, *Trends Pharmacol. Sci.*, 2019, **40**, 747-762.
17. S. Gupta, I. Singh, A. K. Sharma and P. Kumar, *Front. Bioeng. and Biotechnol.,* 2020, **8**.
18. S. Pal, D. Mehta, U. Dasgupta and A. Bajaj, *Biomed. Mater.*, 2021, **16**, 024102.
19. A. K. Das and P. K. Gavel, *Soft Matter*, 2020, **16**, 10065-10095.
20. D. M. Ryan and B. L. Nilsson, *Polym. Chem.*, 2012, **3**, 18-33.
21. E. R. Draper and D. J. Adams, *Chem*, 2017, **3**, 390-410.
22. P. Chakraborty and E. Gazit, *ChemNanoMat*, 2018, **4**, 730-740.
23. R. Schweitzer-Stenner and N. J. Alvarez, *J. of Phys. Chem. B*, 2021, **125**, 6760-6775.
24. J. Y. C. Lim, Q. Lin, K. Xue and X. J. Loh, *Mater. Today Adv.*, 2019, **3**, 100021.
25. M. Criado-Gonzalez, E. Espinosa-Cano, L. Rojo, F. Boulmedais, M. R. Aguilar and R. Hernández, *ACS Appl. Mater. Interfaces*, 2022, **14**, 10068-10080.
26. M. K. Pradhan, D. Gupta, K. R. Namdev, Anjali, C. Miglani, A. Pal and A. Srivastava, *Nanoscale*, 2022, **14**, 15079-15090.
27. T. Mondal, A. Chatterjee, B. Hansda, B. Mondal, P. Sen and A. Banerjee, *Soft Matter*, 2024, **20**, 1236-1244.
28. M. Yi, J. Guo, H. He, W. Tan, N. Harmon, K. Ghebreyessus and B. Xu, *Soft Matter*, 2021, **17**, 8590-8594.
29. T. Das, M. Häring, D. Haldar and D. Díaz Díaz, *Biomater. Sci.*, 2018, **6**, 38-59.
30. Z. Yang, H. Gu, D. Fu, P. Gao, J. K. Lam and B. Xu, *Adv. Mater.*, 2004, **16**, 1440-1444.
31. J. N. Abraham, S. Joseph, R. Trivedi and M. Karle, *Polym. Int.*, 2021, **70**, 222-229.

32. B. D. Gupta, A. Halder, T. Vijayakanth, N. Ghosh, R. Konar, O. Mukherjee, E. Gazit and S. Mondal, *J. Mater. Chem. B*, 2024, **12**, 8444-8453.
33. V. Jayawarna, S. M. Richardson, A. R. Hirst, N. W. Hodson, A. Saiani, J. E. Gough and R. V. Ulijn, *Acta Biomater.*, 2009, **5**, 934-943.
34. D. M. Ryan, S. B. Anderson, F. T. Senguen, R. E. Youngman and B. L. Nilsson, *Soft Matter*, 2010, **6**, 475-479.
35. V. Jayawarna, M. Ali, T. A. Jowitt, A. F. Miller, A. Saiani, J. E. Gough and R. V. Ulijn, *Adv. Mater.*, 2006, **18**, 611-614.
36. K. Tao, A. Levin, L. Adler-Abramovich and E. Gazit, *Chem. Soc. Rev.*, 2016, **45**, 3935-3953.
37. A. Y. Gahane, P. Ranjan, V. Singh, R. K. Sharma, N. Sinha, M. Sharma, R. Chaudhry and A. K. Thakur, *Soft Matter*, 2018, **14**, 2234-2244.
38. E. R. Draper, K. L. Morris, M. A. Little, J. Raeburn, C. Colquhoun, E. R. Cross, T. O. McDonald, L. C. Serpell and D. J. Adams, *CrystEngComm*, 2015, **17**, 8047-8057.
39. Y. Wang, Z. Zhang, L. Xu, X. Li and H. Chen, *Colloids Surf. B Biointerfaces*, 2013, **104**, 163-168.
40. A. Rajbhandary, D. M. Raymond and B. L. Nilsson, *Langmuir*, 2017, **33**, 5803-5813.
41. B. L. Abraham, S. G. Mensah, B. R. Gwinnell and B. L. Nilsson, *Soft Matter*, 2022, **18**, 5999-6008.
42. B. L. Abraham, P. Agredo, S. G. Mensah and B. L. Nilsson, *Langmuir*, 2022, **38**, 15494-15505.
43. M. L. Jagrosse, P. Agredo, B. L. Abraham, E. S. Toriki and B. L. Nilsson, *ACS Biomater. Sci. Eng.*, 2023, **9**, 784-796.
44. D. M. Raymond, B. L. Abraham, T. Fujita, M. J. Watrous, E. S. Toriki, T. Takano and B. L. Nilsson, *ACS Appl. Bio Mater.*, 2019, **2**, 2116-2124.
45. B. O. Okesola, Y. Wu, B. Derkus, S. Gani, D. Wu, D. Knani, D. K. Smith, D. J. Adams and A. Mata, *Chem. Mater.*, 2019, **31**, 7883-7897.
46. B. Giménez-Hernández, E. Falomir and B. Escuder, *ChemBioChem*, 2023, **24**, e202300438.
47. D. M. Ryan, T. M. Doran and B. L. Nilsson, *Chem. Commun.*, 2011, **47**, 475-477.
48. D. M. Ryan, T. M. Doran and B. L. Nilsson, *Langmuir*, 2011, **27**, 11145-11156.
49. W. Liyanage, K. Vats, A. Rajbhandary, D. S. W. Benoit and B. L. Nilsson, *Chem. Commun.*, 2015, **51**, 11260-11263.
50. Y. Tsuji, X. Li and M. Shibayama, *Gels*, 2018, **4**, 50.
51. A. S. Braegelman, R. C. Ollier, B. Su, C. J. Addonizio, L. Zou, S. L. Cole and M. J. Webber, *ACS Appl. Bio Mater.*, 2022, **5**, 4589-4598.
52. B. L. Abraham, E. S. Toriki, N. D. J. Tucker and B. L. Nilsson, *J. Mater. Chem. B*, 2020, **8**, 6366-6377.

DATA AVAILABILITY STATEMENT

TEM and additional oscillatory rheology data are available in the Electronic Supplemental Information file (Supporting Information). Data from oscillatory rheology experimental results presented in Figure 4A, Figure 4B, Figure 4C, Figure 4D, Figure S7A (Supporting Information), Figure S7B (Supporting Information), Figure S8 (Supporting Information), Figure S9 (Supporting Information), Figure S10 (Supporting Information) are included in a second supplemental spreadsheet file entitled “Ghosh Rheology Data 2024.”